Ilter, Mehmet C.; Wichman, Risto; Hamalainen, Jyri; Ikki, Salama

A New Information Harvesting Mechanism for Far-Field Wireless Power Transfer

Published in:
2023 IEEE 97th Vehicular Technology Conference, VTC 2023-Spring - Proceedings

DOI:
10.1109/VTC2023-Spring57618.2023.10201039

Published: 01/01/2023

Document Version
Peer-reviewed accepted author manuscript, also known as Final accepted manuscript or Post-print

A New Information Harvesting Mechanism for Far-Field Wireless Power Transfer

Mehmet C. Ilter, Risto Wichman, Jyri Hämäläinen and Salama Ikki
School of Electrical Engineering, Aalto University, Espoo, Finland
Department of Electrical and Computer Engineering, Lakehead University, Thunder Bay, ON, Canada
Email: {mehmet.ilter, risto.wichman,jyri.hamalainen}@aalto.fi
sikki@lakeheadu.ca

***Abstract*—Considering the current capability in hardware design, the wireless power transmission (WPT) enables the next stage in the current consumer electronics revolution by prolonging the lifetime of devices powered by batteries. Recently, *Information Harvesting* (IH) introduced a novel mechanism for wireless power and information transfer which differs from existing far-field wireless power transfer and simultaneous transmission of power and data protocols. In this paper, a new IH mechanism which relies on quadrature spatial modulation (QSM) is proposed and the simulation results demonstrate that the proposed mechanism improves the secrecy at information receiver and provide more harvested energy to the harvester.**

***Index Terms*—Wireless power and information transfer, information harvesting, information seeding, secrecy capacity.**

I. Introduction

In the sixth generation (6G) era, Internet of Things platforms are required to support massive number of devices and to tackle energy demands in addition to existing challenges of massive data content. Wireless power transfer (WPT) introduces a revolution to consumer electronics by providing ambient energy resources enabling battery-less infrastructures, which can decode the messages, passive RF identification (RFID), and machine-to-machine solutions. Nowadays, zero-power communication technology has also been emerged as the next logical step in the future networks which promises information transmission where its energy is harvested from surrounding radio frequency energy without the need to replace or recharge batteries [1]. From this point of view, the different integrations between WPT systems and wireless communication mechanism seem inevitable in the near-future.

In far-field WPT systems, maximizing RF-to-DC efficiency has been the primary focus at the beginning and from this aspect, rectenna is the principal element in the procedures of converting RF waveforms into dc output power. Furthermore, the efficiency of energy harvesting also depends on the choice of WPT waveform deployed at the wireless power transmitter. For instance, it was shown that deploying a multi-sine waveform increases the efficiency of RF-to-DC conversion, so the output dc power [2]. In addition, it has been shown that with the help of passive reflective intelligent surfaces, the output DC power can be maximized further by jointly designing the active transmit beamformer of the transmitter and the passive reflecting beamformer [3].

Rather than only radiating energy via RF signaling, incorporating data communication into power transfer emerged during the last decade. This is mainly referred as simultaneous wireless information and power transfer (SWIPT) for RF-based systems [4] and as recently simultaneous light information and power transfer (SLIPT) for optical-based ones [5]. In those systems, the power and information components are mostly separable from emitting signals over different domains, which can be the energy domain (power splitting), time domain (time splitting), and space domain (antenna splitting) [6]. From this aspect, a trade-off exists between information transfer and energy transfer in such systems. There is an extensive body of work exploring different preferences out of this trade-off [7] and the simultaneous data and power transmission studies can also be found in commercial RFID systems, particularly from reader to RFID tags [8].

In order to secure ongoing data transmission, it should be kept in mind that most devices are simple nodes having limited computational capabilities, so the complexity of encryption-decryption procedures is beyond their capabilities [9]. Sending information and power at the same time makes the SWIPT mechanism limited in terms of the received power and the circuit complexity. Results in [10] demonstrate that power transfer efficiency drops dramatically over the transmission distance in such systems with security enhancement in the design. To address this, a distributed antenna-based SWIPT protocol was proposed [11]. As an alternative approach, creating a modulation signal through a vacant resource block of communication in an orthogonal frequency division multiplexing (OFDM) block has been also proposed in [12].

In order to prevent power transfer efficiency loss and other security concerns resulting from different sensitivities of energy harvester and communication unit, an alternative approach which enables information transfer on top of existing power transfer without disturbing the ongoing wireless power transfer mechanism, so called *Information Harvesting (IH)*, has been recently proposed in [13]. In this way, without sacrificing the range of power transfer service area, information transfer through WPT can be implemented by encoding the information into indices of transmitter entities as in index modulation. In principle, the IH framework consists of two cycles where information seeding cycle aims to embed the information bits into WPT waveform without any termination or disturbance in

existing harvesting activity and information harvesting cycle refers to sense the variations occurred in information seeding cycle at intended receivers. The generalized space shift keying (GSSK)-based IH mechanism and its performance in terms of secrecy capacity and average harvested power was investigated in [14].

In this paper, a promising variant of conventional spatial modulation (SM), quadrature spatial modulation (QSM) is adopted into the IH mechanism. While the QSM exists in many index modulation based implementations, the technique has been also recently used in next generation concepts: reflective intelligent surface (RIS) assisted ambient backscatter communications [15] and millimeter wave (mmWave) communication [16]. Within the context of IH, the QSM-based implementation activates two layers of antennas to transmit two WPT signals, real and imaginary parts, in one symbol period. For complex waveforms, M-QAM and complex Gaussian signals are utilized and the simulation results show that QSM-based IH favors not only the secrecy perspective of the information receivers but also the amount of harvested energy in energy harvester (EH). Also, the results illustrate that the performance obtained from the proposed mechanism can be improved more with proper selection of the WPT waveform and integration with physical layer security solutions.

II. QSM-BASED INFORMATION HARVESTING MECHANISM

A. WPT transmission model

The proposed mechanism is illustrated in Fig. 1 where the WPT has N_{t} transmit antennas in total and the available information block is mapped into two transmit antenna activation vectors, to determine which N_{a} antennas out of N_t are used for emitting the real and the imaginary parts of the complex power transfer signal such that $N_a \leq N_t$. It was known that the maximum number of information bits, η, can be mapped into the transmit antenna indices for GSSK modulation where a WPT signal is transmitted a chosen set of transmit antenna is expressed as $L = \left\lfloor \log_2 \binom{N_t}{N_a} \right\rfloor$ along with floor operation, $\lfloor \cdot \rfloor$. Under the QSM-based implementation, there exists two transmit antenna vectors where the first transmit antenna vector corresponds to the real part of a wireless power symbol and the second one does the imaginary part so the total number of combinations increases to 2η. Note that since the emitted WPT waveform does not have any information component itself rather than active antenna combination so there is no additional communication transmission over the existing WPT waveform.

Assuming s is a complex WPT signal, $s \in \mathcal{C}$, and its the real part, $\Re\{s\}$, and its imaginary part, $\Im\{s\}$, are transmitted separately through the activated antennas over cosine and sine carriers respectively [17]. Then, the received signal at EH without any additional artificial noise (AN) can be expressed as

$$y_{\mathrm{EH}} = \mathbf{h}_{\mathrm{eh}} \Re\{s\} + i\mathbf{g}_{\mathrm{eh}} \Im\{s\} + \mathbf{n}_e \tag{1}$$

where $\mathbf{h}_{\mathrm{eh}}$ and $\mathbf{g}_{\mathrm{eh}}$ correspond to channel coefficient matrices with the size of $N_a \times N_{\mathrm{eh}}$ of the WPT-EH link for the transmission of $\Re\{s\}$ and $\Im\{s\}$, respectively. Herein, N_{eh} refers to the number of receive antenna at the EH and $\mathbf{n}_e$ in (1) is the complex additive white Gaussian noise (AWGN).

In order to increase the secrecy of WPT-IR channels against eavesdropping activity in a given service area, the WPT can generate artificial noise (AN) on top of its power transfer waveforms and add them to existing transmitting signals. In this way, the jamming signals degrade the received signal quality at Eve without any damage to the IR when the channel state information (CSI) knowledge of IR is available at the WPT which is obtained from the cycle that information receiver initiates the signaling between the WPT and the IR by sending request for information packages [13].

For the AN generation, it is assumed that IR has N_r receive antennas such that $N_r < N_t$. Then, the singular value decomposition (SVD) can be implemented as $\mathbf{H}_{\mathrm{IR}} = \mathbf{U}\mathbf{\Lambda}\mathbf{V}^H$ where $\mathbf{H}_{\mathrm{IR}}$ is a $N_r \times N_t$ channel matrix with $r = \mathrm{rank}\,(\mathbf{H}_{\mathrm{IR}})$ and $\mathbf{V} = [\mathbf{v}_1 \mathbf{v}_2 \dots \mathbf{v}_r \mathbf{v}_{r+1} \dots \mathbf{v}_{N_t}]$ includes the nullspaces of $\mathbf{H}_{\mathrm{IR}}$, which are $\mathbf{V}_\perp = [\mathbf{v}_{r+1} \dots \mathbf{v}_{N_t}]$. Then, the AN-added WPT waveform can be expressed as

$$x = \sum_{i=r+1}^{N_t} \delta_i \mathbf{v}_i u_i. \tag{2}$$

The second term in (2) is the jamming signal obtained from independent identically distributed (i.i.d.) Gaussian distribution, $u_i \sim \mathbb{C}\mathcal{N}\left(0, \lambda_u^2\right)$ along with $\sum_{i=r+1}^{N_t} \delta_i^2 = 1$. Since $\mathbf{H}_{\mathrm{IR}}.\mathbf{V}_\perp = 0$ holds, the generated AN on top of existing WPT waveform does not affect on the received signal in IR while it leads additional jamming power in Eve side due to $\mathbf{H}_{\mathrm{eve}}.\mathbf{V}_\perp \neq 0$. Then, the received signal at EH coupled with AN can be expressed as

$$y_{\mathrm{EH}} = \mathbf{h}_{\mathrm{eh}} \Re\{s\} + i\mathbf{g}_{\mathrm{eh}} \Im\{s\} + \mathbf{H}_{\mathrm{eh}} x + \mathbf{n}_e. \tag{3}$$

Note that the AN is emitted from all available antennas at WPT so $\mathbf{H}_{\mathrm{eh}}$ is $N_t \times N_{\mathrm{eh}}$ channel matrix where $\mathbf{h}_{\mathrm{eh}}$ and $\mathbf{g}_{\mathrm{eh}}$ are the subsets of $\mathbf{H}_{\mathrm{eh}}$.

B. Harvesting model at EH

Once the WPT transmits power transfer waveforms into a service area, the EH is expected to convert (1) into DC-output power thanks to the rectennas. The EH consists of receive antenna chain along with N_{eh} receive antennas, battery charging unit, and battery. Herein, the battery charging unit is configured to establish a link between the receive antenna chain and battery, wherein the manner in which power is transferred from the wireless power transceiver is controlled according to the parameters and/or state information assigned by the power management unit. Note that the fraction of time exists where the rectenna cannot perform harvesting since input RF power lies below certain RF power which is referred as *rectenna sensitivity* and after certain received signal power level at harvester, *rectenna saturation power*, the harvested energy stays constant as shown in [18]. After considering these realistic aspects and harvesting formulation proposed in [19], the output

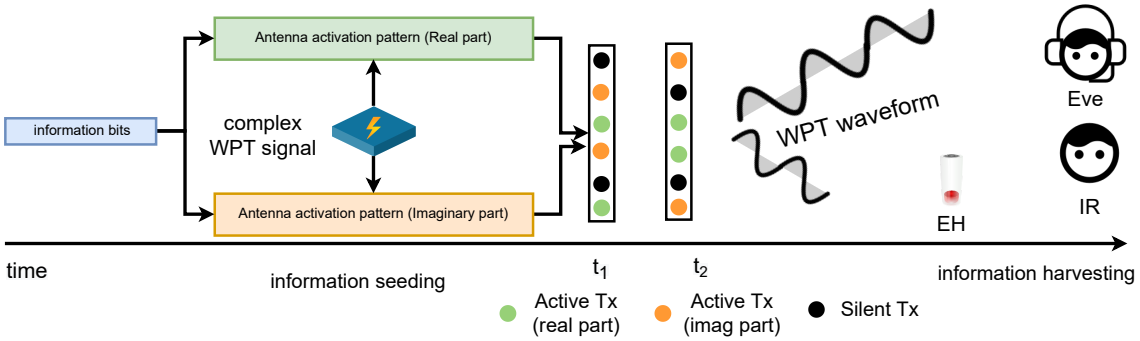

Fig. 1: The illustration of proposed IH mechanism where the QSM-based information seeding and information harvesting cycles are implemented along with $N_t = 6$ and $N_a = 2$ over a service area WPT, EH, IR, and Eve exist.

DC power can be expressed as a function of the received RF signal can be expressed as

$$v_{out} = \begin{cases} 0, & P_r^t \in [0, \Gamma_{in}] \\ \beta_2 P_r^t + \beta_4 {P_r^t}^2, & P_r^t \in [\Gamma_{in}, \Gamma_{sat}] \\ \beta_2 \delta_{sat} + \beta_4 \delta_{sat}^2, & P_r^t \in [\Gamma_{in}, \Gamma_{sat}] \end{cases} \tag{4}$$

where P_r^t is the received input power at time instant t, $P_r^t = |y(t)|^2$, Γ_{in} refers the harvester sensitivity, Γ_{sat} denotes the saturation level and β_2, β_4 are the parameters of the nonlinear rectifier model. Since EHs have multiple receive antennas, DC combining [19] can be utilized where each branch has its own rectifier so that the total DC output power can be obtained from $\sum_{q=1}^{N_{\text{eh}}} v_{out,q}^2 / R_L$ where R_L refers to the resistive load used to determine the output DC power.

C. Decoding mechanism at the IR and the Eve

The goal of the information receiver (IR) is to retrieve the information mapped into active transmit indices so the IR can detect the information bits as in the conventional QSM scheme without performing any symbol decoding. Then maximum likelihood (ML) procedure can be implemented at the IR as

$$\left\langle \hat{h}_{\text{IR}}, \hat{g}_{\text{IR}} \right\rangle = \arg \min_{\mathbf{h}_{\text{IR}}^l, \mathbf{g}_{\text{IR}}^l, l \in L} |y_{\text{IR}} - \mathbf{h}_{\text{IR}}^l \Re\{s\} - i\mathbf{g}_{\text{IR}}^l \Im\{s\}|^2 \tag{5}$$

Herein, $\mathbf{h}_{\text{IR}}^l$ and $\mathbf{g}_{\text{IR}}^l$ correspond to the lth potential codebook channel coefficient set of the WPT-IR link out of L candidates for real part and imaginary part transmission, respectively. $\left\langle \hat{h}_{\text{IR}}, \hat{g}_{\text{IR}} \right\rangle$ refers the estimated indices of active transmit antennas at the IR, for example $\left\langle \hat{h}_{\text{IR}}, \hat{g}_{\text{IR}} \right\rangle = \langle [110], [011] \rangle$ implies the 1st and 2nd transmit antennas are active for $\Re\{\mathbf{s}\}$ and 2nd and 3rd do for $\Im\{\mathbf{s}\}$, respectively.

The similar mechanism can also be adapted to illegitimate information receivers, so-called eavesdroppers. In that case, the decoding at Eve can be expressed

$$\left\langle \hat{h}_{\text{eve}}, \hat{g}_{\text{eve}} \right\rangle = \arg \min_{\mathbf{h}_{\text{eve}}^l, \mathbf{g}_{\text{eve}}^l, l \in L} |y_{\text{eve}} - \mathbf{h}_{\text{eve}}^l \Re\{s\} - i\mathbf{g}_{\text{eve}}^l \Im\{s\}|^2 \tag{6}$$

where $\mathbf{h}_{\text{eve}}^l$ and $\mathbf{g}_{\text{eve}}^l$ correspond to the lth potential codebook channel coefficient set of the WPT-Eve link. The artificial noise can seriously worsen Eve's decoding performance.

III. The Secrecy Analysis

Each transmit antenna set for the real and the imaginary parts is selected with the same probability, $\frac{1}{L}$. Then, the received signal at the IR shows the following distribution [20]

$$\Pr(\mathbf{y}_{\text{IR}}) = \frac{1}{L^2} \sum_{l_1=1}^{L} \sum_{l_2=1}^{L} \frac{1}{\pi\sigma^2} e^{-\frac{||\mathbf{r}_{\text{IR}}||^2}{\sigma^2}} \tag{7}$$

where $\mathbf{r}_{\text{IR}} = y_{\text{IR}} - \mathbf{h}_{\text{IR}}^{l_1} \Re\{s\} - i\mathbf{g}_{\text{IR}}^{l_2} \Im\{s\}$. Then, the mutual information at IR, $\mathcal{I}_{\text{IR}}(\mathbf{r}_{\text{IR}}, \mathbf{h}_{\text{l,eff}})$, can be expressed in (8), which is a special case of [Eq. (14), [20]]. Therein, n_{IR} is the Gaussian noise at the IR and $\mathbf{d}_{l_1,l_2}^{r_1,r_2}$ is defined as

$$\mathbf{d}_{l_1,l_2}^{r_1,r_2} = \mathbf{h}_{\text{IR,eff}}^{l_2} \Re\{s\} + i\mathbf{h}_{\text{IR,eff}}^{l_1} \Im\{s\} - \mathbf{h}_{\text{IR,eff}}^{r_1} \Re\{s\} - i\mathbf{h}_{\text{IR,eff}}^{r_2} \Im\{s\} \tag{10}$$

where $\mathbf{h}_{\text{IR,eff}}^l = \mathbf{h}_{l_1} + \cdots + \mathbf{h}_{l_{N_a}}$ is the effective channel after incorporating only active transmit antenna set at the IR [21]. Similar to (7), the received signal at Eve shows the following distribution [20]

$$\Pr(\mathbf{y}_{\text{eve}}) = \frac{1}{L^2} \sum_{l_1=1}^{L} \sum_{l_2=1}^{L} \frac{1}{\pi\sigma^2} e^{-\frac{||\mathbf{r}_{\text{eve}}||^2}{\sigma^2}} \tag{11}$$

where $\mathbf{r}_{\text{eve}} = y_{\text{eve}} - \mathbf{h}_{\text{eve}}^{l_1} \Re\{s\} - i\mathbf{g}_{\text{eve}}^{l_2} \Im\{s\}$. After taking into account the existence of the AN at Eve side, the mutual information at Eve, $\mathcal{I}_{\text{eve}}(\mathbf{r}_{\text{eve}}, \mathbf{h}_{\text{eve,eff}})$, is given in (9), which is a special case of [Eq. (15), [20]]. Herein, $\delta_{l_1,l_2}^{r_1,r_2}$ can be expressed as

$$\begin{aligned} \delta_{l_1,l_2}^{r_1,r_2} =& \mathbf{C}_\epsilon^{-\frac{1}{2}} \left(\mathbf{g}_{\text{eve,eff}}^{l_2} \Re\{s\} + i\mathbf{g}_{\text{eve,eff}}^{l_1} \Im\{s\} \right) \\ & - \mathbf{C}_\epsilon^{-\frac{1}{2}} \left(\mathbf{g}_{\text{eve,eff}}^{r_1} \Re\{s\} - i\mathbf{g}_{\text{eve,eff}}^{r_2} \Im\{s\} \right) \end{aligned} \tag{12}$$

where $\mathbf{g}_{\text{eve,eff}}^l = \mathbf{g}_{l_1} + \cdots + \mathbf{g}_{l_{N_a}}$ is the effective channel and $\mathbf{C}_\epsilon$ refers a covariance matrix of interference plus noise term at Eve, which is,

$$\mathbf{C}_\epsilon = \frac{\lambda_u^2}{N_t - r} \mathbf{G}_{\text{eve}} \left(\sum_{i=r+1}^{N_t} \mathbf{v}_i \mathbf{v}_i^H \right) \mathbf{H}_{\text{eve}}^H + \lambda^2 \mathbf{I}. \tag{13}$$

$$\mathcal{I}_{\mathrm{IR}}\left(\mathbf{y}_{\mathrm{IR}},\mathbf{h}_{\mathrm{l,eff}}\right)=\log_2\left(L^2\right)-\frac{1}{L^2}\sum_{l_1=1}^{L}\sum_{l_2=1}^{L}\mathbb{E}_{\,\mathbf{n}_{\mathrm{IR}}}\left[\log_2\left(\sum_{r_1=1}^{L}\sum_{r_2=1}^{L}e^{-\frac{1}{\sigma^2}\left\|\mathbf{d}_{l_1,l_2}^{r_1,r_2}+\mathbf{n}_{\mathrm{IR}}\right\|^2-\left\|\mathbf{n}_{\mathrm{IR}}\right\|^2}\right)\right]. \tag{8}$$

$$\mathcal{I}_{\mathrm{eve}}\left(\mathbf{y}_{\mathrm{eve}},\mathbf{h}_{\mathrm{l,eff}}\right)=\log_2\left(L^2\right)-\frac{1}{L^2}\sum_{l_1=1}^{L}\sum_{l_2=1}^{L}\mathbb{E}_{\,\mathbf{n}_{\mathrm{eve}}}\left[\log_2\left(\sum_{r_1=1}^{L}\sum_{r_2=1}^{L}e^{-\frac{1}{\sigma^2}\left\|\delta_{l_1,l_2}^{r_1,r_2}+\mathbf{n}_{\mathrm{eve}}\right\|^2-\left\|\mathbf{n}_{\mathrm{eve}}\right\|^2}\right)\right]. \tag{9}$$

Note that the channel between the WPT and the IR relies on QSM-based GSSK modulated antenna indices so the capacity analysis deducts into a capacity analysis for discrete-input continuous-output memoryless channel (DCMC) [22] and it might be not straightforward to obtain the closed-form analysis in most cases. With the existence of Eve in the service area, the secrecy rate of IH can be expressed as [21]

$$\mathcal{R}_{\mathrm{IH}}=\max\{0,\mathcal{I}_{\mathrm{IR}}\left(\mathbf{y}_{\mathrm{IR}},\mathbf{h}_{\mathrm{l,eff}}\right)-\mathcal{I}_{\mathrm{eve}}\left(\mathbf{y}_{\mathrm{eve}},\mathbf{g}_{\mathrm{l,eff}}\right)\}, \tag{14}$$

Note that positive secrecy from (14) implies communication opportunity on top of existing WPT mechanism even some information can be leaked to Eve in the service area.

IV. Numerical Results

In this section, we would like to investigate the advantages of implementing information seeding mechanism which results from QSM-based IH implementation compared with GSSK-based IH implementation given in [14]. For this purpose, the average harvested power at the EH, the secrecy rates at the IR and bit error rate at IR are used as the performance indicators.

To comply with the maximum EIRP of specified in FCC Title 47, Part 15 regulations [23], the WPT output power, P_T, is set to 36 dBm which is distributed between the generation of the AN and WPT signals, s and x, according to ρ; $\lambda_s^2=(1-\rho)P_T$ and $\lambda_u^2=\rho P_T$. From this aspect, $\rho=0$ corresponds to transmitting the WPT waveform without AN. For the rectenna operation in the simulations, it is assumed that perfect matching and ideal low pass filter exist. Also, the pair of $\{\beta_2,\beta_4\}$ in (4) is considered as $\{0.0034,0.3829\}$, R_L is set to 50Ω [24] and the operation range of the input power of the rectenna is chosen based on PowerCast module [18] such that $\Gamma_{in}=10^{-1.2}$ mW and $\Gamma_{sat}=10$mW in (4). For complex WPT signal, single tone 16-QAM and complex Gaussian signaling are considered as in [3] without incorparating any part of channel information whereas the CSI-adaptive complex WPT signals as given in [25] can be applied as well.

A. EH perspective: PAPR and harvested energy

In this subsection, the channels between the WPT and the EH are modeled with two different Rician parameters, K. The dominant LoS link corresponds to $K=5$ and $K=0$ implies Rayleigh fading model and the following path-loss model is considered; $PL\,[\mathrm{dB}]=35.3+37.6\log_{10}(d)$, where d is the distance between the WPT and an EH in meters.To investigate the effects of adapting QSM into IH mechanism, the variations of the received the peak to average power ratio at EH are initially investigated where the WPT has

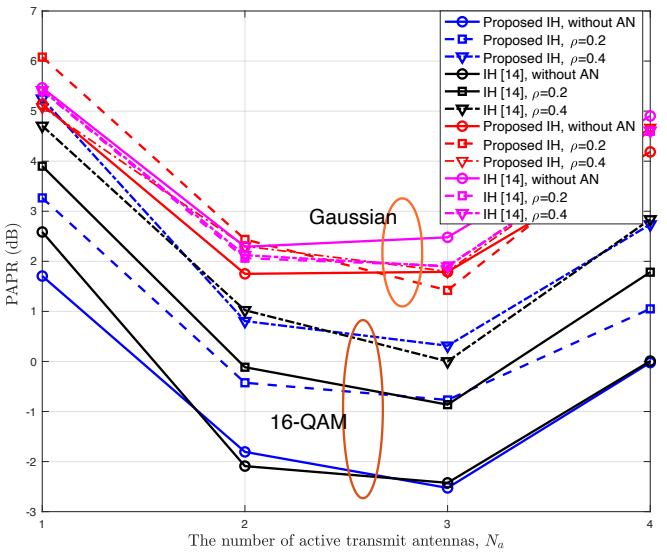

Fig. 2: The received PAPR values at EH with respect to N_a. The EH is located $d=5$m from the WPT where the dominant LoS link exists ($K=5$). Two different complex WPT signals are used for the proposed IH and IH mechanism given in [14]; 16-QAM and Gaussian signal.

$N_t=5$ transmit antennas and N_a antennas are active while an EH performs harvesting at the distance of $d_{\mathrm{eh}}=1$m in the service area . For any far-field power transfer, the characteristic of peak-to-power ratio (PAPR) can give hint about harvested energy amount. Although low PAPR signals are always preferred at the transmitter, it was shown in [19] that high PAPR signals at the input of the energy harvester can result in more harvested power.

From this aspect, the PAPR values of GSSK-based IH in [14] and the proposed IH with respect to different N_a values when the dominant LoS exists are illustrated in Fig. 2. To see the effects of the AN generation at the input of the EH, three ρ values are considered such that $\{0,0.2,0.4\}$ where ρ corresponds to WPT transmission without AN. The IR is assumed to be located $d_{\mathrm{IR}}=3$m which is related with AN generation. As it can be seen from the figure that the proposed QSM-based IH tends to similar received PAPR values for 16-QAM and complex Gaussian signals. In the 16-QAM cases, higher ρ introduces higher PAPR whereas the negligible variations are observed when Gaussian signals are used at the WPT since the AN signal itself consists of the weighted summation of independent Gaussian signals so more powerful AN compensates the portion taken from the power of the intended WPT signal, s.

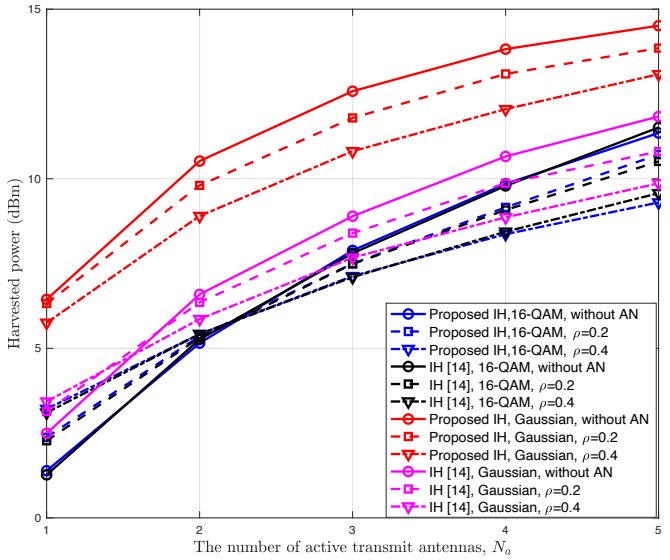

Fig. 3: The harvested power at EH with respect to N_a. The EH is located $d = 5$m from the WPT where the dominant LoS link exists ($K = 5$). Two different complex WPT signals are used for the proposed IH and IH mechanism given in [14]; 16-QAM and Gaussian signal.

Now, the average harvested power at EH is plotted in Fig.3. For 16-QAM cases, the harvested power at EH is similar in both IH mechanisms. Note that although similar levels of PAPR values are observed for each IH mechanim in Fig. 2, the proposed QSM-based IH yields higher harvested power. From this aspect, the combination of Gaussian signaling and QSM-based IH introduces higher average radiated power. In all cases, higher ρ yields lower harvested power regardless of the choice of the WPT signal and higher harvested power can be obtained with higher values N_a.

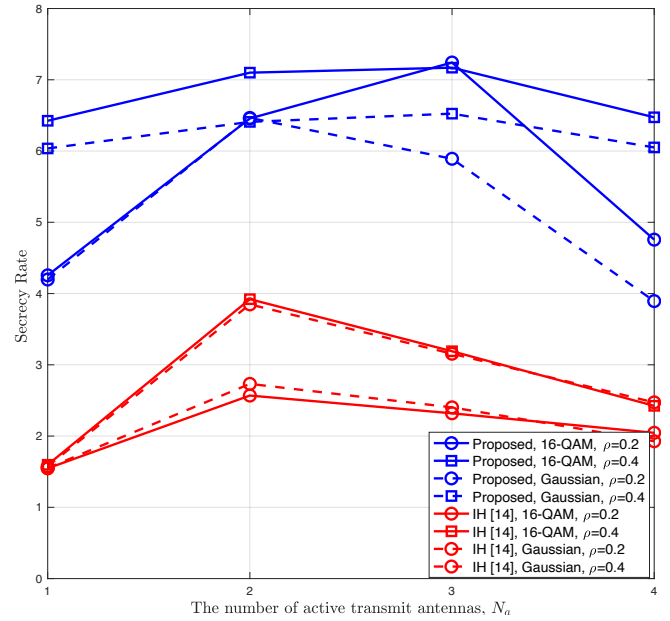

Fig. 4: Simulated secrecy rates at IR with respect to N_a values along with different waveforms and ρ values where the proposed IH and IH mechanism in [14] are considered. The IR has four receive antennas and the Eve has three such that $N_{\mathrm{r}} = 4$ and $N_{\mathrm{eve}} = 3$

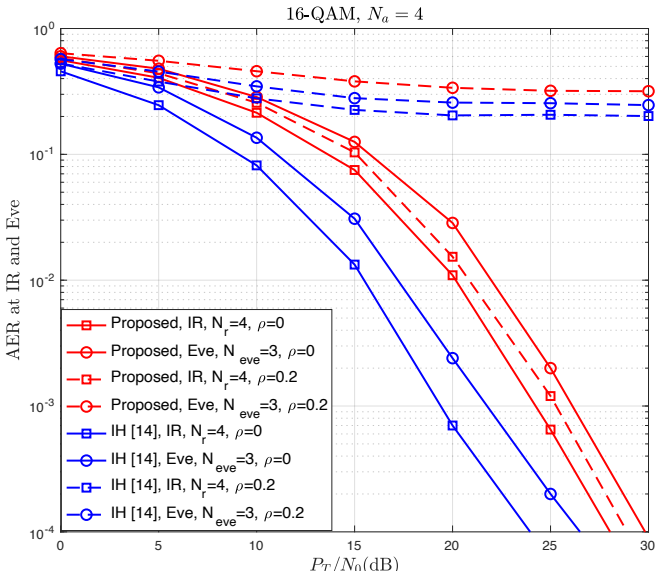

Fig. 5: The simulated AER at the IR with respect to different $SNR = P_T/N_0$ values where the proposed IH and IH mechanism in [14] are considered with 16-QAM waveform over different ρ values. The IR has four receive antennas and the Eve has three such that $N_{\mathrm{r}} = 4$ and $N_{\mathrm{eve}} = 3$.

B. IR perspective: Secrecy rate and antenna error rate (AER)

Now, we investigate the potential benefits of the IH from the IR perspective in terms of the secrecy capacities and antenna error rates (AER). Herein, the calculation of the AER lies on comparing transmit antenna array vector and estimated antenna array vector at IR and Eve. The simulated secrecy rates of the QSM-based IH mechanism and IH mechanism given in [14] with respect to N_a are given in Fig. 4. Without loss of

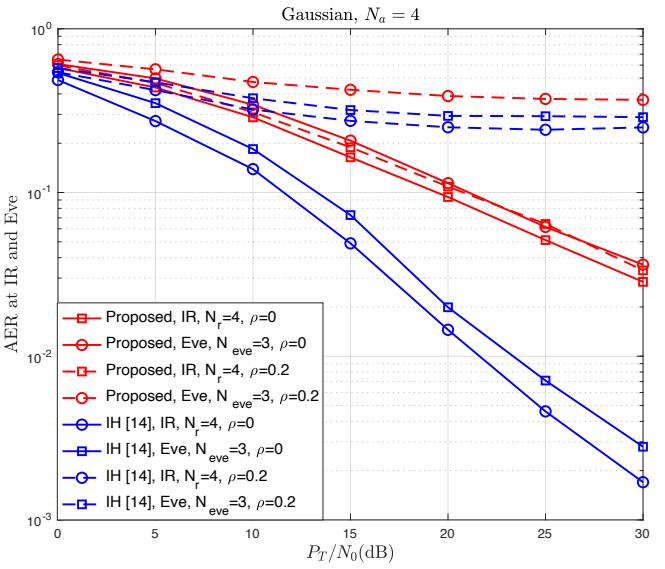

Fig. 6: The simulated AER at the IR with respect to different $SNR = P_T/N_0$ values where the proposed IH and IH mechanism in [14] are considered with Gaussian waveform over different ρ values.The IR has four receive antennas and the Eve has three such that $N_{\mathrm{r}} = 4$ and $N_{\mathrm{eve}} = 3$.

generality, the channels of the WPT-IR and the WPT-Eve are assumed to be unit variance Rayleigh fading channels. For both WPT waveforms, the proposed IH mechanism outperforms the IH mechanism given in [14] and 16-QAM waveform yields better secrecy capacity compared to Gaussian one. In addition, it is observed that the choice of complex WPT signal has more impact on the secrecy rate than the one [14].

After seeing the advantages in terms of secrecy capacity of the proposed IH mechanism, the simulated AER at Bob and Eve are plotted in Fig. 5 and Fig. 6 when 16-QAM and Gaussian signaling are used as WPT signal, respectively. Based on Fig. 3, $N_a = 4$ is assumed to minimize the effects on the harvested energy amount at EH. As it can be seen from Fig. 5, implementing (5) and (6) introduces additional complexity in the decoding the antenna indices so the performance of the proposed QSM-based IH yields higher antenna error rates at the IR and Eve in case of that $\rho = 0$. The advantage of the proposed IH mechansim can be observed when the AN is emitted from WPT with $\rho = 0.2$ where the IR can reach lower AER values with the proposed QSM-based IH mechanism.

In Gaussian signaling scenario, in order to work with a more realistic scenario and fair comparison with 16-QAM, a similar Gaussian frame which has 16 discrete value is repeated by the WPT during a cycle and the frame is assumed to be known in the IR and Eve perfectly. Although higher AER values are observed in Fig. 6 in comparision with 16-QAM cases, the proposed QSM-based IH mechanism performs better than IH mechanism in [14] when the AN exists.

V. Conclusion

The Information Harvesting (IH) was introduced as a novel mechanism which enables data communications on top of existing wireless power transfer over IoT networks. In this paper, a QSM-based IH scheme is proposed and the results show that a new mechanism can improve the secrecy of IH mechanism while increasing the harvested energy in the EH with a proper choice of complex WPT signal. Also, the proposed IH mechanism seems having more capability when combining with physical layer security solutions at the WPT.

Acknowledgment

This study has been supported by the Academy of Finland (grant number 334000).

References

[1] Y. Liu, D. Li, H. Dai, C. Li, and R. Zhang, "Understanding the impact of environmental conditions on zero-power internet of things: An experimental evaluation," *IEEE Wireless Commun.*, pp. 1–8, 2022.

[2] C. R. Valenta and G. D. Durgin, "Rectenna performance under power-optimized waveform excitation," in *IEEE Int. Conf. on RFID (RFID)*, 2013, pp. 237–244.

[3] Q. Yue, J. Hu, K. Yang, and K.-K. Wong, "Intelligent reflecting surface aided wireless power transfer with a DC-combining based energy receiver and practical waveforms," *IEEE Trans. Veh. Technol.*, vol. 71, no. 9, pp. 9751–9764, 2022.

[4] T. D. Ponnimbaduge Perera, D. N. K. Jayakody, S. K. Sharma, S. Chatzinotas, and J. Li, "Simultaneous wireless information and power transfer (SWIPT): Recent advances and future challenges," *IEEE Commun. Surveys Tuts.*, vol. 20, no. 1, pp. 264–302, 2018.

[5] M. Uysal, S. Ghasvarianjahromi, M. Karbalayghareh, P. D. Diamantoulakis, G. K. Karagiannidis, and S. M. Sait, "SLIPT for underwater visible light communications: Performance analysis and optimization," *IEEE Trans. Wireless Commun.*, vol. 20, no. 10, pp. 6715–6728, 2021.

[6] W. Liu, X. Zhou, S. Durrani, and P. Popovski, "SWIPT with practical modulation and RF energy harvesting sensitivity," in *Proc. IEEE Int. Conf. Commun. (ICC)*, 2016, pp. 1–7.

[7] G. Amarasuriya, E. G. Larsson, and H. V. Poor, "Wireless information and power transfer in multiway massive MIMO relay networks," *IEEE Trans. Wireless Commun.*, vol. 15, no. 6, pp. 3837–3855, 2016.

[8] G. Paolini, A. Quddious, D. Chatzichristodoulou, D. Masotti, S. Nikolaou, and A. Costanzo, "An energy-autonomous SWIPT RFID tag for communication in the 2.4 GHz ISM band," in *3rd URSI Atlantic and Asia Pacific Radio Science Meeting (AT-AP-RASC)*, 2022, pp. 1–4.

[9] J. Tournier, F. Lesueur, F. Le Mouël, L. Guyon, and H. Ben-Hassine, "A survey of IoT protocols and their security issues through the lens of a generic IoT stack," *Internet of Things*, p. 100264, 2020.

[10] D. Xu and H. Zhu, "Secure transmission for SWIPT IoT systems with full-duplex IoT devices," *IEEE Internet of Things J.*, vol. 6, no. 6, pp. 10 915–10 933, 2019.

[11] Y. Huang, M. Liu, and Y. Liu, "Energy-efficient SWIPT in IoT distributed antenna systems," *IEEE Internet of Things J.*, vol. 5, no. 4, pp. 2646–2656, 2018.

[12] Y. Nakamoto, N. Hasegawa, T. Hirakawa, and Y. Ohta, "A study on OFDM modulation suitable for wireless power transfer," in *Wireless Power Week (WPW)*, 2022, pp. 21–24.

[13] M. C. Ilter, R. Wichman, M. Säily, and J. Hämäläinen, "Information harvesting for far-field wireless power transfer," *IEEE Internet of Things Magazine*, vol. 5, no. 2, pp. 127–132, 2022.

[14] M. C. Ilter, E. Basar, R. Wichman, and J. Hämäläinen, "Information harvesting for far-field RF power transfer through index modulation," in *Proc. IEEE Glob. Commun. Conf. (GLOBECOM)*, 2022.

[15] A. Bhowal, S. Aïssa, and R. S. Kshetrimayum, "RIS-assisted advanced spatial modulation techniques for ambient backscattering communications," *IEEE Trans. Green Commun. Netw.*, vol. 5, no. 4, pp. 1684–1696, 2021.

[16] A. Basit, W.-Q. Wang, S. Y. Nusenu, and S. Wali, "FDA based QSM for mmwave wireless communications: Frequency diverse transmitter and reduced complexity receiver," *IEEE Trans. Wireless Commun.*, vol. 20, no. 7, pp. 4571–4584, 2021.

[17] R. Mesleh, S. S. Ikki, and H. M. Aggoune, "Quadrature spatial modulation," *IEEE Trans. Veh. Technol.*, vol. 64, no. 6, pp. 2738–2742, 2015.

[18] P. N. Alevizos and A. Bletsas, "Sensitive and nonlinear far-field RF energy harvesting in wireless communications," *IEEE Trans. Wireless Commun.*, vol. 17, no. 6, pp. 3670–3685, 2018.

[19] B. Clerckx, J. Kim, K. W. Choi, and D. I. Kim, "Foundations of wireless information and power transfer: Theory, prototypes, and experiments," *Proc. IEEE Proc.*, vol. 110, no. 1, pp. 8–30, 2022.

[20] Z. Huang, Z. Gao, and L. Sun, "Anti-eavesdropping scheme based on quadrature spatial modulation," *IEEE Commun. Lett.*, vol. 21, no. 3, pp. 532–535, 2017.

[21] Y. Wei, L. Wang, and T. Svensson, "Analysis of secrecy rate against eavesdroppers in MIMO modulation systems," in *Int. Conf. on Wireless Commun. Signal Processing (WCSP)*, 2015, pp. 1–5.

[22] U. Singh, M. R. Bhatnagar, and T. A. Tsiftsis, "Secrecy analysis of SSK modulation: Adaptive antenna mapping and performance results," *IEEE Trans. Wireless Commun.*, vol. 20, no. 7, pp. 4614–4630, 2021.

[23] Federal Commun. Comm., "47 CFR Part15-Radio Frequency Devices," Washington, DC, USA, 2016.

[24] J. Kim, B. Clerckx, and P. D. Mitcheson, "Signal and system design for wireless power transfer: Prototype, experiment and validation," *IEEE Trans. Wireless Commun.*, vol. 19, no. 11, pp. 7453–7469, 2020.

[25] B. Clerckx, A. Costanzo, A. Georgiadis, and N. Borges Carvalho, "Toward 1G mobile power networks: RF, signal, and system designs to make smart objects autonomous," *IEEE Microw. Mag.*, vol. 19, no. 6, pp. 69–82, 2018.